

# A prognostic signature based on the expression profile of the ferroptosis-related long non-coding RNAs in hepatocellular carcinoma

Xixi Lin<sup>1,2,C,D</sup>, Sijie Yang<sup>3,A–C,E,F</sup>

<sup>1</sup> Division of Experimental Radiation Biology, Department of Radiation Therapy, University Hospital Essen, University of Duisburg-Essen, Germany

<sup>2</sup> Department of Radiotherapy, Second Affiliated Hospital of Guangxi Medical University, Nanning, China

<sup>3</sup> Collaborative Innovation Centre of Regenerative Medicine and Medical BioResource Development and Application Co-constructed by the Province and Ministry, Guangxi Medical University, Nanning, China

A – research concept and design; B – collection and/or assembly of data; C – data analysis and interpretation;

D – writing the article; E – critical revision of the article; F – final approval of the article

Advances in Clinical and Experimental Medicine, ISSN 1899–5276 (print), ISSN 2451–2680 (online)

Adv Clin Exp Med. 2022;31(10):1099–1109

## Address for correspondence

Sijie Yang

E-mail: Yangsijiedj@sina.com

## Funding sources

None declared

## Conflict of interest

None declared

Received on January 17, 2022

Reviewed on April 19, 2022

Accepted on April 28, 2022

Published online on May 18, 2022

## Abstract

**Background.** Ferroptosis is a special form of cell death with extensive biological associations with various cancers; however, the role of aberrantly expressed ferroptosis-related long non-coding RNAs (lncRNAs) in hepatocellular carcinoma (HCC) remains unclear.

**Objectives.** To explore the role and prognostic value of ferroptosis-related lncRNAs in HCC and to screen potential therapeutic targets.

**Materials and methods.** The RNA-seq data for 424 HCC patients and clinical data for 377 HCC patients were obtained from The Cancer Genome Atlas (TCGA) and evaluated using the Pearson's test to identify differentially expressed lncRNAs. The univariate analysis, least absolute shrinkage and selection operator Cox regression analysis were performed to construct and validate a prognostic risk-score model. The prognostic capacity was evaluated using the Kaplan–Meier method, univariate and multivariate Cox regression, and receiver operating characteristic (ROC) curve analyses. The enrichment analysis was performed to explore the functions of ferroptosis-related lncRNAs from the perspective of tumor immunology.

**Results.** Seventeen differentially expressed lncRNAs were identified (*AL139384.1*, *AL928654.1*, *MKLN1-AS*, *AC145207.8*, *LINC00205*, *ZFPM2-AS1*, *LINC00942*, *POLH-AS1*, *AC090772.3*, *AL603839.3*, *AC012073.1*, *AC099850.1*, *AC026401.3*, *AP001469.3*, *AL031985.3*, *SNHG10*, *SNHG21*) to establish the risk-score model. Survival analyses demonstrated poorer survival in high-risk patients, and the risk score was shown to be a better independent prognostic factor than conventional clinical characteristics. Additionally, we found close correlations between the risk score and immune cell subpopulation functions, as well as between the expression of immune checkpoint and carcinogenic N6-methyladenosine (m6A)-related mRNAs.

**Conclusions.** The novel ferroptosis-related lncRNA signature may serve as an individualized prognostic prediction tool for patients with HCC.

**Key words:** immune response, hepatocellular carcinoma, long non-coding RNA, ferroptosis, genes

## Cite as

Lin X, Yang S. A prognostic signature based on the expression profile of the ferroptosis-related long non-coding RNAs in hepatocellular carcinoma *Adv Clin Exp Med*. 2022;31(10):1099–1109. doi:10.17219/acem/149566

## DOI

10.17219/acem/149566

## Copyright

Copyright by Author(s)

This is an article distributed under the terms of the Creative Commons Attribution 3.0 Unported (CC BY 3.0) (<https://creativecommons.org/licenses/by/3.0/>)

## Background

Hepatocellular carcinoma (HCC) is the main subtype of primary liver cancer and the 4<sup>th</sup> most common cause of cancer-related deaths worldwide.<sup>1</sup> The incidence of HCC in USA increased from 4.4/100,000 in 2000 to 6.7/100,000 in 2012.<sup>2</sup> Multidisciplinary treatment strategies have greatly improved the efficacy of HCC treatment, while novel immunotherapy and molecular targeted therapies, such as programmed cell death protein 1 inhibitors, have shown promising results in selected patients.<sup>3,4</sup> However, the survival outcomes of patients with advanced HCC remain poor, with a 5-year overall survival (OS) rate <30%.<sup>5,6</sup> Thus, there is a need to identify novel potential therapeutic targets and accurate prognostic biomarkers at the gene level.

Mounting evidence has indicated the involvement of ferroptosis, a special mode of programmed cell death, in several pathophysiological processes of HCC.<sup>7</sup> Ferroptosis is characterized by the over-accumulation of lethal reactive oxygen species (ROS) and production of lipid peroxides,<sup>8</sup> and has shown suppressive effects in head and neck, colorectal and ovarian cancer.<sup>9–11</sup> In the context of HCC, ferroptosis induced by the multikinase inhibitor sorafenib and its potential targets has attracted the attention of researchers. Louandre et al. demonstrated that the deactivation of retinoblastoma protein has increased the efficacy of sorafenib in HCC by exacerbating ferroptosis, both in vitro and in vivo.<sup>12</sup> Additionally, Sun et al. found that the expression of metallothionein-1G after sorafenib treatment contributed to drug resistance and negatively regulated ferroptosis.<sup>13</sup> The increasing appreciation of the importance of ferroptosis in terms of the pathogenesis and treatment of HCC highlights the need to understand the mechanisms underlying ferroptosis-related genetic alterations in HCC.

Long non-coding RNAs (lncRNAs) perform a wide range of regulatory functions at the gene expression level. They have been shown to play a vital role in promoting the progression of HCC through the involvement in proliferative signaling, invasion and metastasis, angiogenesis, as well as immune escape.<sup>14</sup> Recent studies have indicated the potential role of lncRNAs in regulating ferroptotic cell death in relation to cancer biology. For example, the overexpression of lncRNA *H19* was reported to function as a competing endogenous RNA to enhance the activity of ferroptosis.<sup>15</sup> These findings suggest that the ferroptosis–lncRNA relationship may have relevant and important functions in terms of prognostic prediction and treatment in patients with HCC.

## Objectives

The role of ferroptosis-related lncRNAs is currently not fully understood and sequence-based systematic evaluations has been limited. We therefore aimed to explore

the role and prognostic value of ferroptosis-related lncRNAs in HCC by constructing a lncRNA signature based on the Cancer Genome Atlas (TCGA), thereby screening potential targets for HCC treatment.

## Materials and methods

### Data collection

Transcriptome data for 424 HCC patients (374 tumor and 50 non-cancerous (normally differentiated)) and clinicopathological data for 377 HCC patients (age, sex, tumor grade, TNM stage, follow-up time, and survival outcome) were obtained from the TCGA-HCC database up to October 1, 2021. The clinical characteristics of patients are shown in Table 1. The corresponding ferroptosis-related genes were downloaded from FerrDb database (<http://www.zhounan.org/ferrdb/>; the first database dedicated to ferroptosis regulators and ferroptosis-disease associations).<sup>16</sup> Free data on gene regulators, including drivers, suppressors and markers, could be downloaded for further management and investigation. We identified a total of 382 genes (drivers: 150; suppressors: 109; markers: 123; detailed data given in Supplementary Table 1). The correlations between lncRNAs and HCC were analyzed using the Pearson's test. We first evaluated the functions of the ferroptosis-related differentially expressed genes (DEGs), and then assessed the related biological pathways with Gene Ontology analysis, and analyzed biological processes (BP), molecular functions (MF), and cellular components (CC) regulated by the DEGs using Kyoto Encyclopedia of Genes and Genomes (KEGG) analysis, using R software (ggplot2 package; R Foundation for Statistical Computing, Vienna, Austria).

**Table 1.** Clinical characteristics of patients in The Cancer Genome Atlas (TCGA) dataset

Variable	Number of samples
Gender (male/female)	255/122
Age [years] ( $\leq 65$ / $> 65$ /NA)	235/141/1
Grade (G1/G2/G3/G4/NA)	55/180/124/13/5
Stage (I/II/III/IV/NA)	175/87/86/5/24
T (T1/T2/T3/T4/NA)	185/95/81/13/3
M (M0/M1/NA)	272/4/101
N (N0/N1/NA)	257/4/116

NA – not applicable.

### Construction of ferroptosis-related lncRNA prognostic signature

We identified the ferroptosis-related lncRNA signature using univariate Cox regression analyses, least absolute shrinkage and selection-penalized Cox regression.

The risk scores were calculated as the sum of coefficient lncRNA  $\times$  expression of lncRNA. The HCC patients were divided into high-risk and low-risk group according to the median risk score, and we compared the OS between the 2 groups using the Kaplan–Meier analysis, and evaluated the prognostic capacity of the risk-score model using receiver operating characteristic (ROC) curves.

## Gene set enrichment analysis and predictive nomogram

We performed gene set enrichment analysis (GSEA) to assess the enriched pathways and to define the lncRNA signature with the KEGG gene set. A nomogram combining the prognostic signatures was created to predict the 1-, 3- and 5-year OS of HCC patients.

## Gene expression and immunity analysis

We compared the TMER, CIBERSORT, CIBERSORT-ABS, QUANTISEQ, MCPOUNTER, XCELL, EPIC, and single-sample GSEA (ssGSEA) algorithms (<http://timer.comp-genomics.org/>) to estimate cellular immune responses and cellular components between the low-risk and high-risk group according to the risk score. The tumor-infiltrating immune cell subgroups were quantified using ssGSEA and the immunological functions were assessed. A box diagram was used to assess the differential expression of N6-methyladenosine (m6A)-related genes.

## Statistical analyses

Data were analyzed using Bioconductor packages (R software v. 4.1.0; R Foundation for Statistical Computing). Gene expression was compared between normal and HCC tissues using the Wilcoxon test, and correlations between lncRNAs and HCC were analyzed using the Pearson's test (correlation coefficient  $R^2 > 0.4$  at  $p < 0.01$ ). We identified the differential expression of lncRNAs using the Benjamini–Hochberg method, with the criteria of a false discovery rate  $<0.05$  and  $\log^2$  fold change  $\geq 1$ . We compared the ssGSEA-normalized HCC DEGs with a genome using the Gene Set Variation Analysis (GSVA) R-package. The sensitivity and specificity of the prognostic signature were assessed using ROC and decision curve analyses,<sup>17</sup> and the associations between lncRNAs and clinical characteristics were evaluated with logistic regression analyses and a heatmap graph. The survival of HCC patients based on the ferroptosis-related signature was evaluated using Kaplan–Meier survival analysis with a 2-sided log-rank test. Additionally, immune cell infiltration, immune checkpoint and m6A-related gene expression were compared between the groups using Wilcoxon test. Statistical significance was set at  $p < 0.05$  unless otherwise noted.

## Results

### Enrichment analysis of ferroptosis-related genes

We identified 84 ferroptosis-related DEGs, including 71 upregulated and 13 downregulated genes, using KEGG-based analysis. Among these, BP-related genes were involved with organic acid transport and oxidative stress reaction, as well as changes in nutrient levels, toxic substances and extracellular stimuli. The CC-related genes were primarily related to the nicotinamide adenine dinucleotide phosphate hydrate (NADPH) oxidase complex, apical plasma membrane synthesis pathway, lysosomes, and melanin granules, while the MF were connected to the regulation of NADPH production, along with the binding of molecular oxygen and ferric iron (Supplementary Figure 1A). The KEGG-based analysis indicated that the overexpressed genes were commonly involved in ferroptosis, hypoxia-inducible factor-1 (HIF-1) signaling pathway, multiple cancers, synthesis of microRNAs in cancer cells, diabetes, atherosclerosis, viral infection, endocrine system, cell senescence, leukemia, and the mechanistic target of rapamycin signaling pathway (Supplementary Figure 1B).

### Prognostic signature of ferroptosis-based lncRNAs

A total of 781 ferroptosis-related lncRNAs, including 17 downregulated and 764 upregulated lncRNAs, were found. Sixty-six significant ferroptosis-related lncRNAs that were incorporated into the multivariate Cox analysis were also analyzed using the univariate Cox analysis. Seventeen differentially expressed lncRNAs were finally confirmed as independent prognosis predictors of HCC: *AL139384.1*, *AL928654.1*, *MKLN1-AS*, *AC145207.8*, *LINC00205*, *ZFPM2-AS1*, *LINC00942*, *POLH-AS1*, *AC090772.3*, *AL603839.3*, *AC012073.1*, *AC099850.1*, *AC026401.3*, *AP001469.3*, *AL031985.3*, *SNHG10*, and *SNHG21* (Supplementary Table 2). The network diagram shows the relationship between mRNAs and lncRNAs (Supplementary Figure 1C). On the basis of these findings, we established risk scores and prognostic signatures for the lncRNAs.

### Survival results and multivariate analysis

The Kaplan–Meier analysis indicated that the expression of a high-risk lncRNA signature was related to lower survival outcomes ( $p < 0.001$ ; Fig. 1A). Similar results were obtained in a subgroup analysis according to tumor stage (Supplementary Figure 2A). The area under the ROC curve for the lncRNA signature was higher than those for the clinical indices (Fig. 1B) in all patients, and in subgroups according to tumor stage (Supplementary Figure 2B). The risk survival status plot (Fig. 1C) verified

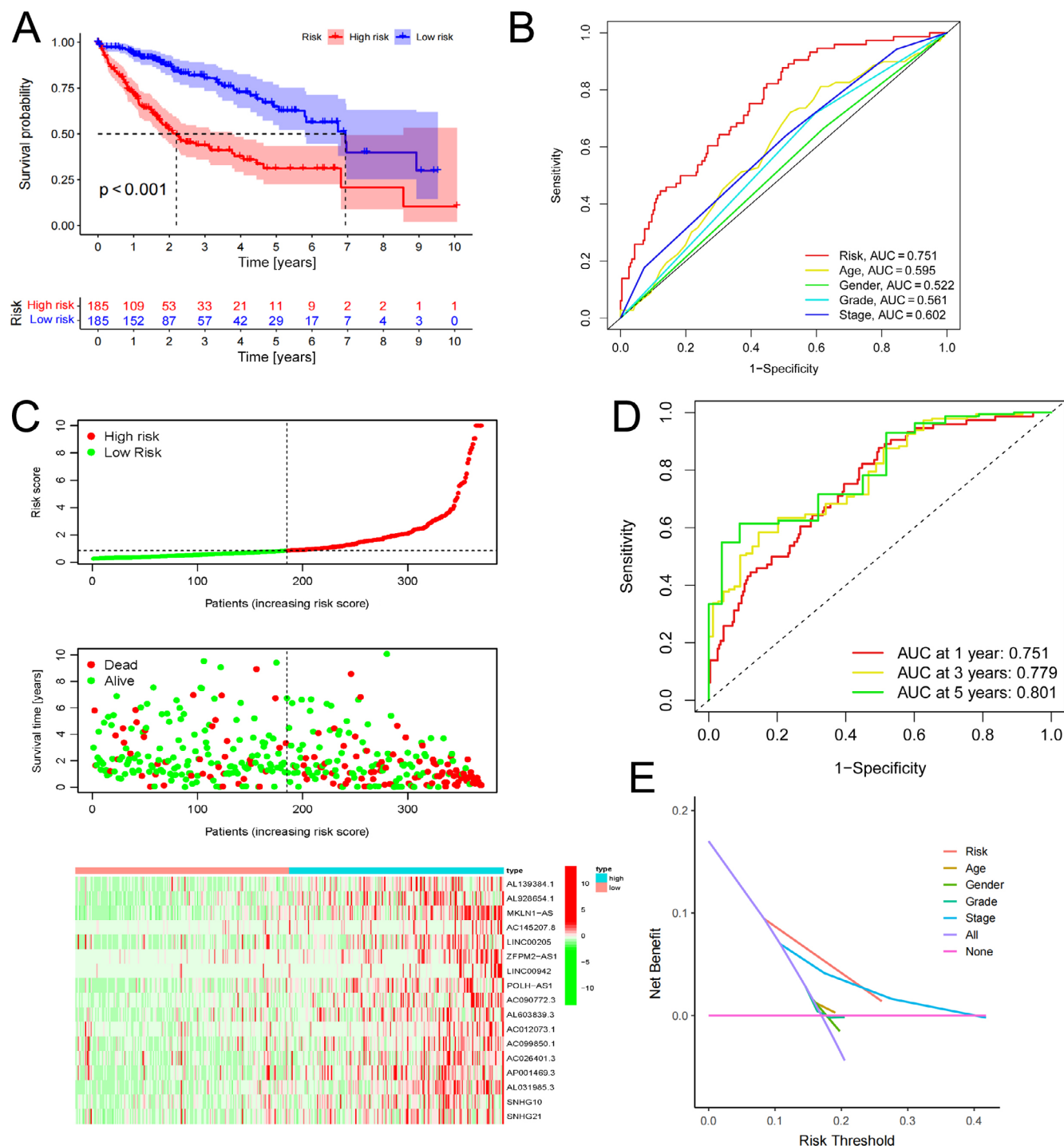


**Fig. 1.** Ferroptosis-related long non-coding RNAs (lncRNAs) signature based on The Cancer Genome Atlas (TCGA). A. Kaplan-Meier curves result. Curves were compared using the log-rank test, hazard ratio (HR) = 3.187 (95% confidence interval (95% CI): 2.245–4.523),  $p = 5.621 \times 10^{-11}$ ; B. The area under the curve (AUC) values of the risk factors in predicting 1-year survival of hepatocellular carcinoma (HCC); C. Risk survival status plot. The high-risk group was related to low survival, and the novel lncRNAs are positively correlated with the risk score; D. The AUC of predicting 1-, 3- and 5-year OS of HCC patients; E. The decision curve analysis (DCA) of the risk factors

that patients with high-risk scores were prone to low survival outcomes. Additionally, the heatmap demonstrated that most candidate lncRNAs were strongly expressed in the high-risk group (Fig. 1C). Taken together, the current risk model demonstrated that specific ferroptosis-associated lncRNAs provided a useful prognostic signature for HCC.

The areas under the curve for 1-, 3- and 5-year OS rates predicted by the novel lncRNA signature were 0.751, 0.779 and 0.801, respectively (Fig. 1D). The signature still exhibited good specificity and sensitivity when analyzed in relation to HCC stage (Supplementary Figure 2C). The decision curve analysis confirmed that the lncRNA signature performed better predictive

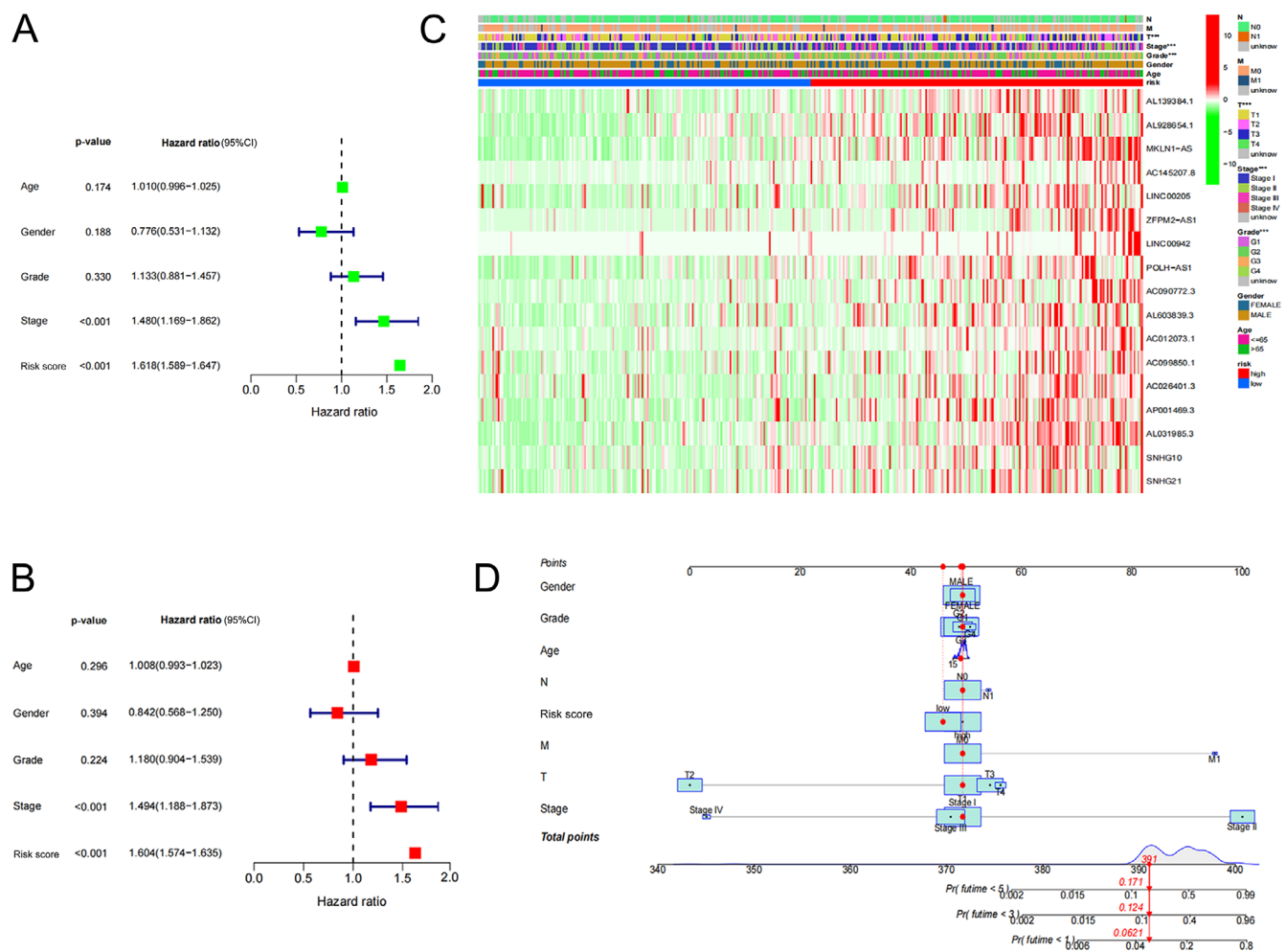


**Fig. 2.** Univariate (A) and multivariate Cox (B) analyses for the expression of ferroptosis-related long non-coding RNAs (lncRNAs; 95% confidence interval (95% CI)); C: Heatmap for ferroptosis-related lncRNAs prognostic signature and clinical manifestations; D: Nomogram for both clinical manifestations and prognostic ferroptosis-related lncRNAs. The points for each of the 8 variables are obtained by drawing a line upwards from the value of each variable to the points line. The sum of points for the 8 variables is marked in the total points line, and the line drawn perpendicularly downward indicates the probability of survival at 1 year, 3 years and 5 years

ability than other conventional clinical and pathological characteristics (Fig. 1E).

The univariate analysis revealed that lncRNA-based signature (hazard ratio (HR): 1.618, 95% confidence interval (95% CI): 1.589–1.647) together with tumor stage (HR: 1.480, 95% CI: 1.169–1.862) were independent prognostic factors for HCC (Fig. 2A, Supplementary Table 3). The multivariate Cox analysis confirmed that the lncRNA signature was an independent prognostic risk factor for HCC (Fig. 2B, Supplementary Table 3).

Heatmap analyses illustrated the association between the prognostic signature of ferroptosis-related lncRNA and clinical manifestations (Fig. 2C). Predictors in the hybrid nomogram incorporated the risk-score model and clinicopathological characteristics (Fig. 2D).

## GSEA

The GSEA revealed that most of the prognostic signatures played roles in metabolism and tumor-related

pathways, including the metabolism of amino acids, salts and drugs (such as  $\beta$ -alanine), butanoate, fatty acids, propanoate, pyruvate, and tryptophan, as well as being involved in the citrate cycle, tricarboxylic acid cycle, complement and coagulation cascades, and the peroxisome proliferator-activated receptor signaling pathway (Supplementary Figure 3).

## Immunity and gene expression

We evaluated the immune response using the MCP-COUNTER, XCELL, EPIC, TIMER, CIBERSORT, CIBERSORT-ABS, and QUANTISEQ algorithms to determine the association between the ferroptosis-related lncRNA signature and tumor immunity (Fig. 3A). The heatmap demonstrated that macrophage and T cell functions were relatively active in the high-risk group. We further investigated the association between immune cell subpopulations and their related functions, and found that the immune cell functions of antigen-presenting cell (APC) co-inhibition, chemokine



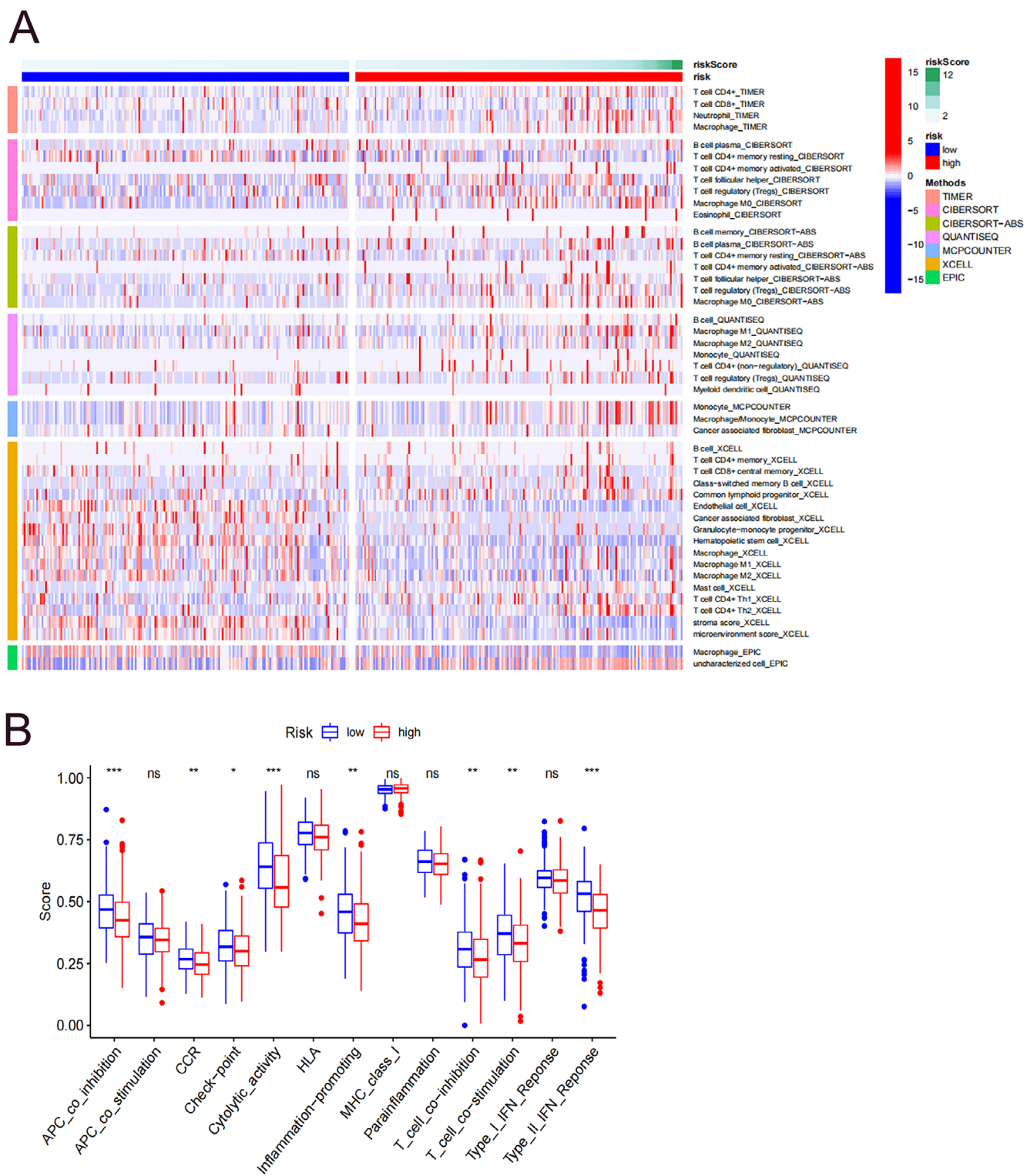
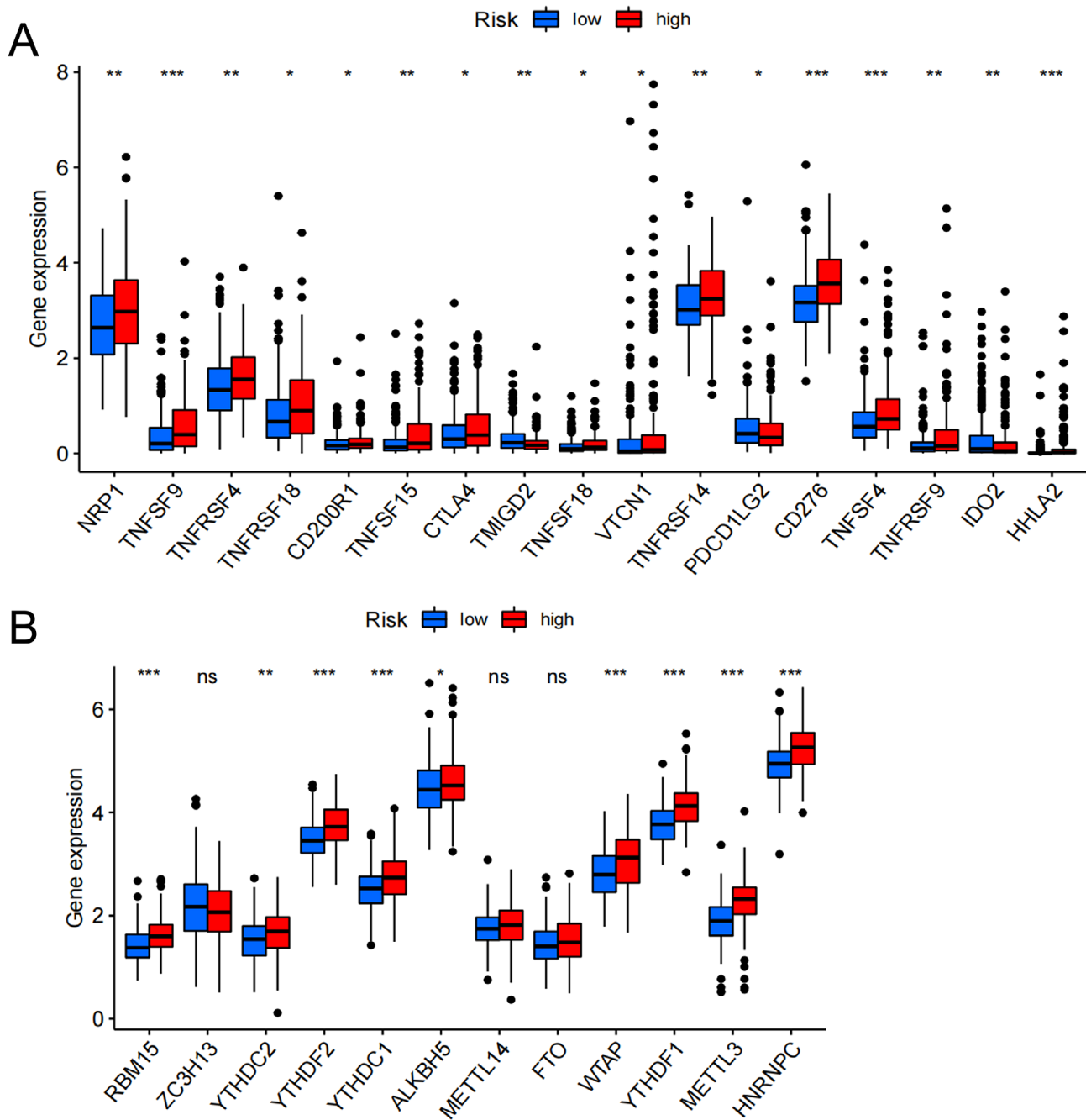


Fig. 3. A. Heatmap for immune responses in the high-risk and low-risk group; B. Single sample gene set enrichment analysis (ssGSEA) for the association between immune cell subpopulations and related functions

\*  $p < 0.05$ , \*\*  $p < 0.01$ , \*\*\*  $p < 0.001$ . The boxes show the middle scores ranging between the 25<sup>th</sup> and 75<sup>th</sup> percentile. The upper and lower whiskers represent scores outside the middle 50% (i.e., the lower 25% of scores and the upper 25% of scores). Values outside this range are considered to be outliers and are represented by dots; APC – antigen-presenting cell; CCR – chemokine receptor; HLA – human leukocyte antigen; MHC – major histocompatibility complex.

receptor (CCR), checkpoint, cytolytic activity, inflammation-promoting, T cell co-inhibition/stimulation, and type II interferon response differed significantly between the high-risk and low-risk group (Fig. 3B, Supplementary Table 4).

Because immune checkpoint inhibition is an important clinical therapeutic strategy in HCC, we also compared the expression of immune checkpoints between the 2 groups.<sup>3,4</sup> All selected immune checkpoints showed



**Fig. 4.** A. Expression of immune checkpoints in the high-risk and low-risk group; B. The expression of N6-methyladenosine (m6A)-related genes in the high-risk and low-risk group

\*  $p < 0.05$ , \*\*  $p < 0.01$ , \*\*\*  $p < 0.001$ . The boxes show the middle scores ranging between the 25<sup>th</sup> and 75<sup>th</sup> percentile. The upper and lower whiskers represent scores outside the middle 50%. Values outside this range are considered to be outliers and are represented by dots.

a significantly differential expression between the 2 groups (Fig. 4A, Supplementary Table 5). Notably, the expression levels of the tumor necrosis factor superfamily (TNFSF)/TNF receptor superfamily (TNFRSF) signaling pathways were all higher in the high-risk group, as compared with the low-risk group.

The m6A as the cofactor of lncRNAs in regulating post-transcriptional modifications has recently come to the spotlight in lncRNA studies.<sup>18</sup> We compared the m6A-related mRNA status between the 2 groups and

found that the expression levels of *RBM15*, *YTHDF1/2*, *ALKBH5*, *WTAP*, *METTL3*, *HNRNPC*, and *YTHDC1/2* were all significantly higher in the high-risk group (Fig. 4B, Supplementary Table 6).

## Discussion

The poor survival and high recurrence rate of HCC have highlighted the need for effective prognostic biomarkers

and therapeutic targets. In this study, we constructed a novel ferroptosis-related lncRNA prognostic risk model and explored the roles of the relevant lncRNAs in the immune response and checkpoint regulation in HCC. These findings allowed us to screen possible ferroptosis-related biomarkers and treatment targets, which might inform the development of new therapeutic approaches.

The prognostic model in our study integrated 17 ferroptosis-related lncRNAs. A subset of lncRNAs (*MKLN1-AS*, *LINC00205*, *ZFPM2-AS1*) was reported to be involved in several HCC cellular activities, including cell proliferation, migration and invasion, cell cycle progression, and apoptosis, through microRNAs, signaling pathways and other biological components or proteins (Table 2). Notably, the biological functions of some of the identified lncRNAs

(*LINC00205*, *ZFPM2-AS1*, *LINC00942*) have also been associated with other malignancies and might thus be non-specific to HCC.<sup>22–24,27–30,33,34</sup> However, numerous other lncRNAs (*AL139384.1*, *AL928654.1*, *AC145207.8*, *POLH-AS1*, *AC090772.3*, *AL603839.3*, *AC012073.1*, *AC099850.1*, *AC026401.3*, *AP001469.3*, *AL031985.3*, *SNHG10*, *SNHG21*) lack corresponding basic studies to validate their prognostic roles in the development of HCC. Further studies are therefore needed to establish the associations of these identified lncRNAs with ferroptosis and their contribution to the regulation of HCC pathogenesis through ferroptosis.

Based on the risk-score method, the ferroptosis-related lncRNA signature classified HCC patients into high-risk and low-risk groups, with significantly different OS rates. Both univariate and multivariate Cox regression analyses

**Table 2.** Biological functions of identified long non-coding RNAs (lncRNAs) in ferroptosis, hepatocellular carcinoma (HCC) and other cancer pathologies

Identified lncRNAs	In other cancer pathology	In HCC pathology
MKLN1-AS	–	<ul style="list-style-type: none"> <li>mediates the effects of SOX9 on the proliferation and EMT of HCC cells<sup>19</sup>;</li> <li>enhances tumor growth in vivo through regulating miR-22-3p/ETS1 axis<sup>20</sup>;</li> <li>positively modulates YAP1 expression and intensifies the proliferation, migration and invasion of HCC cells.<sup>21</sup></li> </ul>
LINC00205	<ul style="list-style-type: none"> <li>enhances hepatoblastoma progression by regulating <i>ROCK1</i> expression via sponging miR-154-3p through MAPK signaling<sup>22</sup>;</li> <li>promotes tumorigenesis and metastasis by competitively suppressing miRNA-26a in gastric cancer<sup>23</sup>;</li> <li>facilitates malignant phenotypes in lung cancer by recruiting FUS to stabilize CSDE1.<sup>24</sup></li> </ul>	<ul style="list-style-type: none"> <li>activated by YY-1, facilitates the proliferation of HCC cells through YY1/miR-26a-5p/CDK6<sup>25</sup>;</li> <li>enhances tumorigenicity of HCC cells through modulating EPHX1 and inhibiting miR-184.<sup>26</sup></li> </ul>
ZFPM2-AS1	<ul style="list-style-type: none"> <li>promotes retinoblastoma progression by targeting miR-511-3p/PAX6 axis<sup>27</sup>;</li> <li>exerts oncogenic effect in cutaneous malignant melanoma progression via targeting miR-650/NOTCH1 signaling<sup>28</sup>;</li> <li>promotes esophageal squamous cell carcinoma (ESCC) cell growth and upregulates TRAF4 to trigger NF-κB pathway by sequestering miR-3612<sup>29</sup>;</li> <li>regulates gastric cancer progression via protecting the degradation of MIF and destabilizing p53.<sup>30</sup></li> </ul>	<ul style="list-style-type: none"> <li>promotes proliferation, migration and invasion by adsorbing miR-576-3p and upregulating HIF-1α<sup>31</sup>;</li> <li>enhances the progression of HCC by competitively binding to miR-139 and downregulating the expression of <i>GDF10</i>.<sup>32</sup></li> </ul>
LINC00942	<ul style="list-style-type: none"> <li>recruits METTL14 to stabilize CXCR4 and CYP1B1 through methylation modification in breast cancer cell proliferation and progression<sup>33</sup>;</li> <li>accelerates chemoresistance in gastric cancer by suppressing MSI2 degradation to stabilize c-Myc mRNA.<sup>34</sup></li> </ul>	–
AL139384.1	–	–
AL928654.1	–	–
AC145207.8	–	–
POLH-AS1	–	–
AC090772.3	–	–
AL603839.3	–	–
AC012073.1	–	–
AC099850.1	–	–
AC026401.3	–	–
AP001469.3	–	–
AL031985.3	–	–
SNHG10	–	–
SNHG21	–	–

EMT – epithelial–mesenchymal transition; MIF – macrophage migration inhibitory factor.



identified the risk score as an independent prognostic factor. Additionally, ROC curve and nomogram analyses showed that the risk score had higher sensitivity and better clinical applicability than traditional standards for predicting HCC survival. Furthermore, stratification analyses by stage confirmed the prognostic predictive value of the risk score signature for each tumor stage.

Numerous studies have established the role of the lncRNA prognostic signature for HCC using bioinformatics analysis. The biological processes related to the lncRNAs in the signatures in these studies included pyroptosis,<sup>35</sup> hypoxia,<sup>36</sup> metabolism,<sup>37</sup> and epithelial–mesenchymal transition.<sup>38</sup> Chen et al. recently reported a ferroptosis-related signature model that integrated both mRNAs and lncRNAs,<sup>39</sup> with outstanding HCC predictive efficiency. Notably, lncRNA *ZFPM2-AS1* was also included in this signature, indicating its strong connection with the development and progression of HCC. In the current study, we focused solely on ferroptosis-related lncRNAs and attempted to explore their role from the perspective of the immune response, immune checkpoints and m6A status.

Mounting evidence has revealed that crosstalk between lncRNAs and immune cells modulates the tumor immune response. However, both immune response and enrichment analyses revealed no significant differences in activities of any immune cell species between the high-risk and low-risk groups. Moreover, levels of all examined immune cell subpopulations were relatively lower in the high-risk group, suggesting a possible regulatory role for lncRNAs in escape from tumor immunity.

Notably, the expression levels of all the immune checkpoints examined in this study were significantly higher in the high-risk group. Among these, TNFSF/TNFRSF signaling pathways showed potential as immunotherapy targets in combination with ferroptosis induction. Interactions among TNFSF/TNFRSF mediate signaling that controls immune cell survival, proliferation and differentiation.<sup>40</sup> As the most important superfamily member, the function of tumor necrosis factor alpha (TNF- $\alpha$ ) in promoting tumor growth and its association with a poor prognosis of HCC have been widely demonstrated, and TNF- $\alpha$  inhibition has accordingly demonstrated appreciable anti-tumor effects in various studies.<sup>41–44</sup> Therefore, the relationship between ferroptosis and TNF- $\alpha$  signaling, as well as the combined efficacy of TNF- $\alpha$  inhibition and ferroptosis in HCC, warrant further investigation.

The importance of reversible chemical modifications of RNA, particularly methylation, has recently gained a renewed interest. The m6A is the most prevalent form of internal mRNA modification and has been implicated in HCC carcinogenesis.<sup>45</sup> Accordingly, the current study showed that several m6A-related genes were highly expressed in the high-risk group (*RBM15*, *YTHDF1/2*, *ALKBH5*, *WTAP*, *METTL3*, *HNRNPC*, and *YTHDC1/2*). The *METTL3* was reported to process oncogenic functions

in HCC by promoting m6A modification of the tumor suppressor gene *SOCS2* in a *YTHDF2*-dependent pathway.<sup>46</sup> At the same time, *METTL3* was shown to work collaboratively with *YTHDF1* to activate the protein translation of Snail, leading to increased epithelial–mesenchymal transition and metastasis of HCC.<sup>47</sup> The investigation of the biological links between m6A and lncRNAs suggests that the modification of m6A might affect the structure, stability, expression, and subcellular distribution of lncRNAs, thereby promoting tumor growth.<sup>48–50</sup> From this perspective, we hope that these findings might identify feasible targets for HCC intervention.

## Limitations

This study had some limitations. It was based mainly on integrative bioinformatics, and histological examination of corresponding tissue samples, follow-up clinical data and experimental validation of the findings are currently lacking. Additionally, the biological functions of the signature components might be nonspecific to HCC, given that they have also been associated with other malignancies. Therefore, further validation of the clinical applicability and clarification of the exact role of ferroptosis in HCC based on our risk score are needed.

## Conclusions

In summary, we constructed a ferroptosis-related lncRNA signature to predict the prognosis of HCC. These results might provide new indications for understanding the mechanisms of ferroptosis-related lncRNAs in regulating the immune response, and for the development of individualized treatments.

## Supplementary materials

The supplementary tables and figures are available at <https://doi.org/10.5281/zenodo.6492096>. The package contains the following files:

Supplementary Figure 1. Gene Ontology (GO), KEGG analysis of DEGs, and the relationship between identified lncRNAs and mRNAs expression.

Supplementary Figure 2. Kaplan–Meier analysis and the area under the curve (AUC) predicting value results of HCC patients in TNM stage I, II and III.

Supplementary Figure 3. GSEA for ferroptosis-related lncRNAs based on TCGA.

Supplementary Table 1. Information of driver, marker and suppressor.

Supplementary Table 2. Statistical information on univariate and multivariate Cox analysis of identified lncRNAs.

Supplementary Table 3. Statistical information on univariate and multivariate Cox analysis of clinical characteristics and the risk score.


Supplementary Table 4. Statistical information on immune function between the high-risk and low-risk group.

Supplementary Table 5. Statistical information on immune checkpoint between the high-risk and low-risk group.

Supplementary Table 6. Statistical information on m6A-related gene expression between the high-risk and low-risk group.

## ORCID iDs

Xixi Lin  <https://orcid.org/0000-0002-3161-0253>

Sijie Yang  <http://orcid.org/0000-0002-4856-8717>

## References

- Yang JD, Hainaut P, Gores GJ, Amadou A, Plymoth A, Roberts LR. A global view of hepatocellular carcinoma: Trends, risk, prevention and management. *Nat Rev Gastroenterol Hepatol*. 2019;16(10):589–604. doi:10.1038/s41575-019-0186-y
- White DL, Thrift AP, Kanwal F, Davila J, El-Serag HB. Incidence of hepatocellular carcinoma in all 50 United States, from 2000 through 2012. *Gastroenterology*. 2017;152(4):812–820.e5. doi:10.1053/j.gastro.2016.11.020
- Pinato DJ, Cortellini A, Sukumaran A, et al. PRIME-HCC: Phase Ib study of neoadjuvant ipilimumab and nivolumab prior to liver resection for hepatocellular carcinoma. *BMC Cancer*. 2021;21(1):301. doi:10.1186/s12885-021-08033-x
- Bang YJ, Golan T, Dahan L, et al. Ramucirumab and durvalumab for previously treated, advanced non-small-cell lung cancer, gastric/gastro-oesophageal junction adenocarcinoma, or hepatocellular carcinoma: An open-label, phase Ia/b study (JVDJ). *Eur J Cancer*. 2020;137:272–284. doi:10.1016/j.ejca.2020.06.007
- Rahimi RS, Trotter JF. Liver transplantation for hepatocellular carcinoma: Outcomes and treatment options for recurrence. *Ann Gastroenterol*. 2015;28(3):323–330. PMID:26130250. PMID:PMCID:PMC4480168.
- Koh YX, Tan HL, Lye WK, et al. Systematic review of the outcomes of surgical resection for intermediate and advanced Barcelona Clinic Liver Cancer stage hepatocellular carcinoma: A critical appraisal of the evidence. *World J Hepatol*. 2018;10(6):433–447. doi:10.4254/wjh.v10.i6.433
- Sun X, Ou Z, Chen R, et al. Activation of the p62-Keap1-NRF2 pathway protects against ferroptosis in hepatocellular carcinoma cells: Hepatobiliary malignancies. *Hepatology*. 2016;63(1):173–184. doi:10.1002/hep.28251
- Yang WS, Stockwell BR. Ferroptosis: Death by lipid peroxidation. *Trends Cell Biol*. 2016;26(3):165–176. doi:10.1016/j.tcb.2015.10.014
- Sui X, Zhang R, Liu S, et al. RSL3 drives ferroptosis through GPX4 inactivation and ROS production in colorectal cancer. *Front Pharmacol*. 2018;9:1371. doi:10.3389/fphar.2018.01371
- Carbone M, Melino G. Stearoyl CoA desaturase regulates ferroptosis in ovarian cancer offering new therapeutic perspectives. *Cancer Res*. 2019;79(20):5149–5150. doi:10.1158/0008-5472.CAN-19-2453
- Shin D, Kim EH, Lee J, Roh JL. Nrf2 inhibition reverses resistance to GPX4 inhibitor-induced ferroptosis in head and neck cancer. *Free Radic Biol Med*. 2018;129:454–462. doi:10.1016/j.freeradbiomed.2018.10.426
- Louandre C, Marcq I, Bouhhal H, et al. The retinoblastoma (Rb) protein regulates ferroptosis induced by sorafenib in human hepatocellular carcinoma cells. *Cancer Lett*. 2015;356(2):971–977. doi:10.1016/j.canlet.2014.11.014
- Sun X, Niu X, Chen R, et al. Metallothionein-1G facilitates sorafenib resistance through inhibition of ferroptosis. *Hepatology*. 2016;64(2):488–500. doi:10.1002/hep.28574
- Wong LS, Wong CM. Decoding the roles of long noncoding RNAs in hepatocellular carcinoma. *Int J Mol Sci*. 2021;22(6):3137. doi:10.3390/ijms22063137
- Zhang R, Pan T, Xiang Y, et al. Curcumenol triggered ferroptosis in lung cancer cells via lncRNA H19/miR-19b-3p/FTH1 axis. *Bioact Mater*. 2022;13:23–36. doi:10.1016/j.bioactmat.2021.11.013
- Zhou N, Bao J. FerrDb: A manually curated resource for regulators and markers of ferroptosis and ferroptosis-disease associations. *Database (Oxford)*. 2020;2020:baaa021. doi:10.1093/database/baaa021
- Vickers AJ, Elkin EB. Decision curve analysis: A novel method for evaluating prediction models. *Med Decis Making*. 2006;26(6):565–574. doi:10.1177/0272989X06295361
- Chen M, Wong CM. The emerging roles of N6-methyladenosine (m6A) deregulation in liver carcinogenesis. *Mol Cancer*. 2020;19(1):44. doi:10.1186/s12943-020-01172-y
- Guo C, Zhou S, Yi W, et al. SOX9/MKL1-AS axis induces hepatocellular carcinoma proliferation and epithelial-mesenchymal transition [published online ahead of print on February 9, 2022]. *Biochem Genet*. 2022. doi:10.1007/s10528-022-10196-6
- Pan G, Zhang J, You F, et al. ETS Proto-oncogene 1-activated muskellin 1 antisense RNA drives the malignant progression of hepatocellular carcinoma by targeting miR-22-3p to upregulate ETS proto-oncogene 1. *Bioengineered*. 2022;13(1):1346–1358. doi:10.1080/21655979.2021.2017565
- Guo C, Zhou S, Yi W, et al. Long non-coding RNA muskellin 1 antisense RNA (MKL1-AS) is a potential diagnostic and prognostic biomarker and therapeutic target for hepatocellular carcinoma. *Exp Mol Pathol*. 2021;120:104638. doi:10.1016/j.yexmp.2021.104638
- Liu G, Zhu Q, Wang H, Zhou J, Jiang B. Long non-coding RNA Linc00205 promotes hepatoblastoma progression through regulating microRNA-154-3p/Rho-associated coiled-coil Kinase 1 axis via mitogen-activated protein kinase signaling. *Aging*. 2022;14(4):1782–1796. doi:10.18632/aging.203902
- Huangfu L, Fan B, Wang G, et al. Novel prognostic marker LINC00205 promotes tumorigenesis and metastasis by competitively suppressing miRNA-26a in gastric cancer. *Cell Death Discov*. 2022;8(1):5. doi:10.1038/s41420-021-00802-8
- Xie P, Guo Y. LINC00205 promotes malignancy in lung cancer by recruiting FUS and stabilizing CSDE1. *Biosci Rep*. 2020;40(10):BSR20190701. doi:10.1042/BSR20190701
- Cheng T, Yao Y, Zhang S, et al. LINC00205, a YY1-modulated lncRNA, serves as a sponge for miR-26a-5p facilitating the proliferation of hepatocellular carcinoma cells by elevating CDK6. *Eur Rev Med Pharmacol Sci*. 2021;25(20):6208–6219. doi:10.26355/eurev.202110\_26991
- Long X, Li Q, Zhi L, Li J, Wang Z. LINC00205 modulates the expression of EPHX1 through the inhibition of miR-184 in hepatocellular carcinoma as a ceRNA. *J Cell Physiol*. 2020;235(3):3013–3021. doi:10.1002/jcp.29206
- Ni W, Li Z, Ai K. lncRNA ZFPM2-AS1 promotes retinoblastoma progression by targeting microRNA miR-511-3p/paired box protein 6 (PAX6) axis. *Bioengineered*. 2022;13(1):1637–1649. doi:10.1080/21655979.2021.2021346
- Liu W, Hu X, Mu X, et al. ZFPM2-AS1 facilitates cell proliferation and migration in cutaneous malignant melanoma through modulating miR-650/NOTCH1 signaling. *Dermatol Ther*. 2021;34(2):e14751. doi:10.1111/dth.14751
- Sun G, Wu C. ZFPM2-AS1 facilitates cell growth in esophageal squamous cell carcinoma via up-regulating TRAF4. *Biosci Rep*. 2020;40(4):BSR20194352. doi:10.1042/BSR20194352
- Kong F, Deng X, Kong X, et al. ZFPM2-AS1, a novel lncRNA, attenuates the p53 pathway and promotes gastric carcinogenesis by stabilizing MIF. *Oncogene*. 2018;37(45):5982–5996. doi:10.1038/s41388-018-0387-9
- Song Y, Jin X, Liu Y, et al. Long noncoding RNA ZFPM2-AS1 promotes the proliferation, migration, and invasion of hepatocellular carcinoma cells by regulating the miR-576-3p/HIF-1α axis. *Anticancer Drugs*. 2021;32(8):812–821. doi:10.1097/CAD.0000000000001070
- He H, Wang Y, Ye P, et al. Long noncoding RNA ZFPM2-AS1 acts as a miRNA sponge and promotes cell invasion through regulation of miR-139/GDF10 in hepatocellular carcinoma. *J Exp Clin Cancer Res*. 2020;39(1):159. doi:10.1186/s13046-020-01664-1
- Sun T, Wu Z, Wang X, et al. Correction to: LNC942 promoting MET-IL14-mediated m6A methylation in breast cancer cell proliferation and progression. *Oncogene*. 2022;41(11):1677–1677. doi:10.1038/s41388-022-02194-0
- Zhu Y, Zhou B, Hu X, et al. lncRNA LINC00942 promotes chemoresistance in gastric cancer by suppressing MSI2 degradation to enhance c-Myc mRNA stability. *Clin Transl Med*. 2022;12(1):e703. doi:10.1002/ctm2.703
- Liu ZK, Wu KF, Zhang RY, et al. Pyroptosis-related lncRNA signature predicts prognosis and is associated with immune infiltration in hepatocellular carcinoma. *Front Oncol*. 2022;12:794034. doi:10.3389/fonc.2022.794034

36. Cheng M, Zhang J, Cao PB, Zhou GQ. Prognostic and predictive value of the hypoxia-associated long non-coding RNA signature in hepatocellular carcinoma. *Yi Chuan*. 2022;44(2):153–167. doi:10.16288/j.yczz.21-416
37. Wang W, Deng Z, Jin Z, et al. Bioinformatics analysis and experimental verification of five metabolism-related lncRNAs as prognostic models for hepatocellular carcinoma. *Medicine (Baltimore)*. 2022;101(4):e28694. doi:10.1097/MD.00000000000028694
38. Tao H, Zhang Y, Yuan T, et al. Identification of an EMT-related lncRNA signature and LINC01116 as an immune-related oncogene in hepatocellular carcinoma. *Aging*. 2022;14(3):1473–1491. doi:10.18632/aging.203888
39. Chen ZA, Tian H, Yao DM, Zhang Y, Feng ZJ, Yang CJ. Identification of a ferroptosis-related signature model including mRNAs and lncRNAs for predicting prognosis and immune activity in hepatocellular carcinoma. *Front Oncol*. 2021;11:738477. doi:10.3389/fonc.2021.738477
40. Dostert C, Grusdat M, Letellier E, Brenner D. The TNF family of ligands and receptors: Communication modules in the immune system and beyond. *Physiol Rev*. 2019;99(1):115–160. doi:10.1152/physrev.00045.2017
41. Jing Y, Sun K, Liu W, et al. Tumor necrosis factor- $\alpha$  promotes hepatocellular carcinogenesis through the activation of hepatic progenitor cells. *Cancer Lett*. 2018;434:22–32. doi:10.1016/j.canlet.2018.07.001
42. Xu ZW, Yan SX, Wu HX, Zhang Y, Wei W. Angiotensin II and tumor necrosis factor- $\alpha$  stimulate the growth, migration and invasion of BEL-7402 cells via down-regulation of GRK2 expression. *Digest Liver Dis*. 2019;51(2):263–274. doi:10.1016/j.dld.2018.06.007
43. Wang H, Liu J, Hu X, Liu S, He B. Prognostic and therapeutic values of tumor necrosis factor- $\alpha$  in hepatocellular carcinoma. *Med Sci Monit*. 2016;22:3694–3704. doi:10.12659/MSM.899773
44. Xiao Y, Huang S, Qiu F, et al. Tumor necrosis factor  $\alpha$ -induced protein 1 as a novel tumor suppressor through selective downregulation of CSNK2B blocks nuclear factor- $\kappa$ B activation in hepatocellular carcinoma. *EBioMedicine*. 2020;51:102603. doi:10.1016/j.ebiom.2019.102603
45. Chen M, Wong CM. The emerging roles of N6-methyladenosine (m6A) deregulation in liver carcinogenesis. *Mol Cancer*. 2020;19(1):44. doi:10.1186/s12943-020-01172-y
46. Chen M, Wei L, Law CT, et al. RNA N6-methyladenosine methyltransferase-like 3 promotes liver cancer progression through YTHDF2-dependent posttranscriptional silencing of SOCS2. *Hepatology*. 2018;67(6):2254–2270. doi:10.1002/hep.29683
47. Lin X, Chai G, Wu Y, et al. RNA m6A methylation regulates the epithelial mesenchymal transition of cancer cells and translation of Snail. *Nat Commun*. 2019;10(1):2065. doi:10.1038/s41467-019-09865-9
48. Brown JA, Kinzig CG, DeGregorio SJ, Steitz JA. Methyltransferase-like protein 16 binds the 3'-terminal triple helix of MALAT1 long noncoding RNA. *Proc Natl Acad Sci U S A*. 2016;113(49):14013–14018. doi:10.1073/pnas.1614759113
49. Zuo X, Chen Z, Gao W, et al. M6A-mediated upregulation of LINC00958 increases lipogenesis and acts as a nanotherapeutic target in hepatocellular carcinoma. *J Hematol Oncol*. 2020;13(1):5. doi:10.1186/s13045-019-0839-x
50. Wu Y, Yang X, Chen Z, et al. m6A-induced lncRNA RP11 triggers the dissemination of colorectal cancer cells via upregulation of Zeb1. *Mol Cancer*. 2019;18(1):87. doi:10.1186/s12943-019-1014-2